

Determination of the Small Band Gap of Carbon Nanotubes Using the Ambipolar Random Telegraph Signal

Fei Liu,* Mingqiang Bao, and Kang L. Wang

Device Research Laboratory, Department of Electrical Engineering, University of California at Los Angeles, Los Angeles, California 90095-1594

Xiaolei Liu, Chao Li, and Chongwu Zhou

Department of Electrical Engineering, University of Southern California, Los Angeles, California 90089

Received March 24, 2005; Revised Manuscript Received May 19, 2005

ABSTRACT

The ambipolar random telegraph signal (RTS) (i.e., RTS in both hole conduction at negative gate biases and electron conduction at positive gate biases) is observed in an ambipolar carbon nanotube field-effect transistor (CNT-FET). Then, the ambipolar RTS is used to extract the small band gap of the SWNT. The determination of the small band gap CNT using RTS demonstrates a potentially high accuracy and stability. Other methods are provided to confirm the small band gap of the SWNT.

The band structures of single-walled carbon nanotubes (SWNTs) have been studied extensively both theoretically and experimentally.¹ It is shown that SWNTs made from perfect grapheme can be clarified into three types: metallic, semiconducting, and small band gap SWNTs. The small band gap SWNTs have their chiralities (m, n) satisfy $m - n = 3 \times \text{integral}$. The curvature-induced hybridization can be attributed to a small band gap.² Furthermore, it is predicted theoretically that defects inside the SWNTs can modify the global band structure of the SWNTs. For example, semiconducting SWNTs can be metallized by a single pentagon–heptagon to close the band gap, depending on the defect density and defect location.³ However, an accurate determination of the ultrasmall band gap of SWNTs in experiments is difficult to make because of the far-infrared setup;⁴ in addition, the measured signal is extremely small because of the small volume of a single SWNT. Alternatively, a zero source–drain bias conductance measurement or a small source–drain current measurement is used to obtain the small band gap of the SWNTs.^{5–7} In these methods, the gate efficiency factor (i.e., $\Delta E_F/\Delta V_g$) needs to be acquired so as to extract the band gap information. Because the modeling of CNT-FETs is still in its developing stage, the gate efficiency factor is often obtained from a separate Coulomb blockade experiment, which results in complication and inaccuracy of the band gap information.

Because of the ultrasmall diameters of carbon nanotubes, they are sensitive to individual charges. Recently, we observed a random telegraph signal (RTS) (i.e., jumping of current/conductance in p-type carbon nanotube backside gate field-effect transistors (FETs) with a high signal-to-noise ratio). This phenomenon is attributed to the charging and discharging of a single defect/atom inside the gate dielectric or in the interface of the gate dielectric.⁸ The single defects or atoms are located outside of the CNTs and do not change the band structure of the CNTs. In this letter, an ambipolar RTS is observed in an ambipolar SWNT FET. The ambipolar RTS mechanism is explained on the basis of the thermionic emission model. After that, we propose to use the ambipolar RTS for the determination of the small band gap of the SWNT. The advantage and reliability of the RTS method are discussed.

SWNTs were synthesized by using a standard chemical vapor deposition (CVD) method as described in ref 9. The SWNTs usually have diameters of 1–3 nm and lengths on the order of 4–5 μm . CNT-FETs are backside gated with a 500 nm thermal oxide layer on top of a highly doped p-type silicon substrate. Ti/Au is used for the metal source and drain contacts. Figure 1 shows the source–drain current (a) and conductance (b) (obtained by a standard lock-in technique) of the CNT-FET measured at a temperature of 4.2 K. The conducting characteristics (i.e., both electron and hole conduction) are observed with the gate voltage scanning from –15 to 15 V. It is interesting to observe that an RTS happens

* Corresponding author. E-mail: feiliu@ee.ucla.edu.

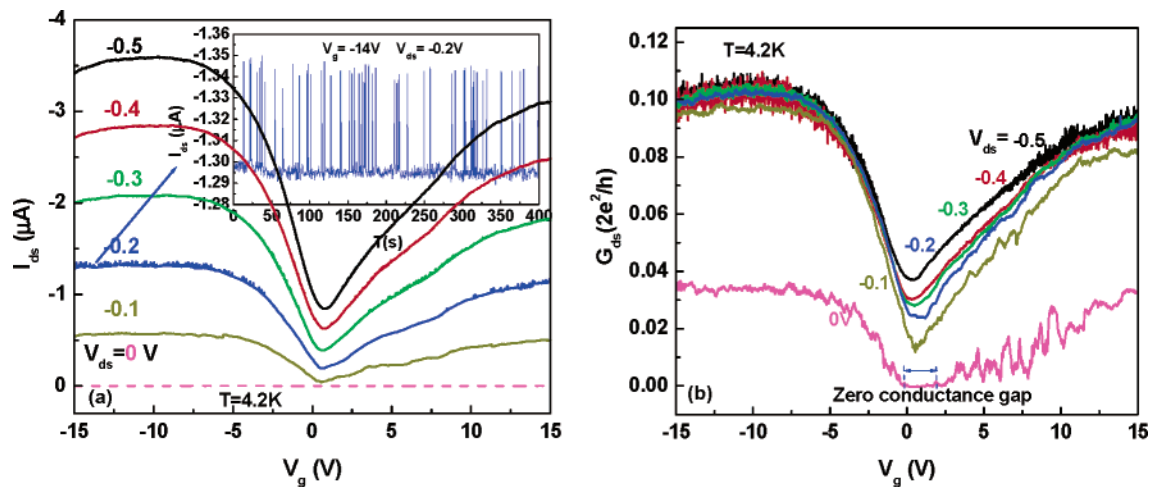


Figure 1. (a) Current as a function of V_g at $T = 4.2$ K for different V_{ds} biases. The inset shows the time-dependent RTS at $V_g = -14$ V and $V_{ds} = -0.2$ V. (b) Corresponding conductance measured simultaneously with the current.

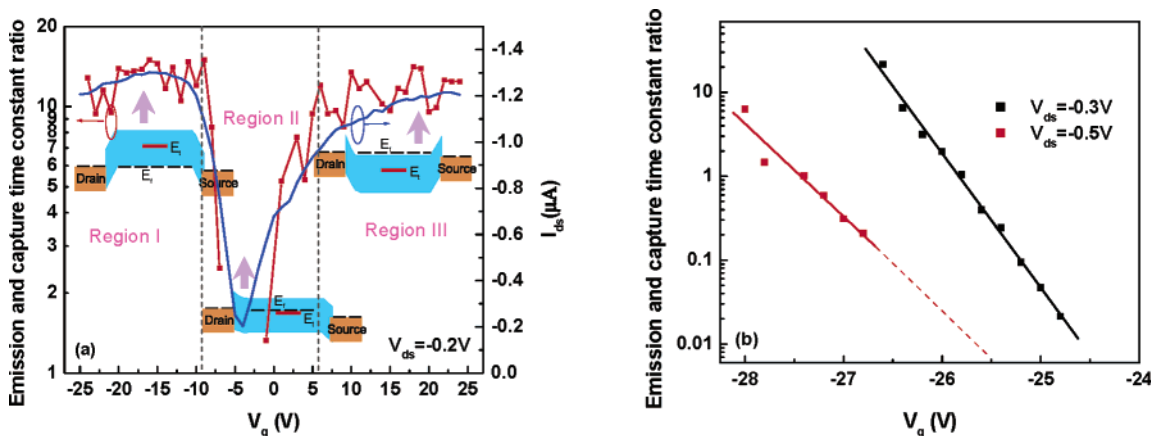


Figure 2. (a) Emission–capture ratio and average source–drain current with respect to gate voltage. The ratio does not change for large positive and negative gate biases. The insets use energy band diagrams to show the principle of using RTS in the ambipolar CNT-FET for the SWNT band gap measurement. (b) RTS emission and capture ratios as a function of gate bias of another device with the same device geometry but a large band gap measured at 4.2 K with different source–drain biases.

over the entire gate scanning range. The inset of Figure 1a shows the time dependence of the RTS source–drain current for a gate bias of -14 V and a source–drain bias of -0.2 V.

The emission and capture time constants ratios, as depicted in Figure 2, are obtained by counting up and down events of RTS for different gate biases.¹⁰ Furthermore, the average source–drain current over a 400 s measurement time slot is plotted in Figure 2 for reference. The RTS is present over a large range of gate bias (from -25 to 25 V), and more interesting is that the RTS occurs both in electron transport (positive gate bias) and hole transport (negative gate bias) in the ambipolar CNT-FET.¹¹ For a large, negative gate bias (< -9 V) in region I, the CNT-FET works as a p-type FET with the Fermi level inside the valance band of CNT as shown on the left side of Figure 2. The probability of finding the CNT-FET in the high absolute current state is lower than that in the low absolute current state, indicating that the defect level is above the CNT Fermi level and, as a result, most of time the defect level has an extra positive charge (hole). In this range, it seems that the capture/emission times and their ratios remain almost unchanged by applying a greater

negative gate bias. Thus, the relative energy position of the CNT Fermi level and the defect level does not change in this gate bias range. It may be concluded that the defect is most likely located at the interface of the CNT and/or very close to the CNT channel. With a smaller negative gate bias, the capture/emission time constants, their ratios, and the average source–drain current change dramatically, as shown in the middle of Figure 2 (region II). First, the Fermi energy of the CNT moves toward the conduction band of the CNT in this gate voltage range, and the emission and capture ratio changes according to the relative energy difference between the defect energy level and the Fermi energy

$$\frac{\tau_c}{\tau_e} = g \exp\left(\frac{E_t - E_f}{k_B T}\right) \quad (1)$$

where τ_c and τ_e are the defect capture and emission time constants; g is the trap degeneracy; E_t is the defect energy; E_f is the Fermi energy of the SWNT; and T is the carrier temperature. Second, when the Fermi energy level lies inside the CNT band gap, the hole density decreases so that the capture time constant increases as seen below

$$\tau_c = \frac{1}{n v_{th} \sigma} \quad (2)$$

where n is the carrier density; v_{th} is the thermal velocity; and σ is the capture cross section. A further increase of the gate positive bias will move the Fermi level into the conduction band and turn the CNT-FET on for electron conduction as shown on the right side of Figure 2a (region III). The similar $I-V$ characteristics and RTS behavior for both electron and hole transport indicate that a similar mechanism occurs for electron conduction. The data suggest that the defect energy level lies roughly in the middle of the band gap. The fact that the large current is observed for both hole and electron conduction means that the Fermi energy is moving from the valence band to the conduction band as the gate bias varies. As the Fermi level moves into the band edge by the bias, further increases of the bias do not move the Fermi level significantly because of the presence of the density of states.¹² Thus, the band gap of the CNT can be extracted by using eq 1 from the emission and capture ratio at large positive and negative gate biases

$$E_g = k_B T \left(\ln \left(\frac{\tau_c}{\tau_c} \right)_{ne} + \ln \left(\frac{\tau_c}{\tau_c} \right)_{po} \right) \quad (3)$$

where E_g is the band gap of the CNT, $(\tau_c/\tau_c)_{ne}$ is the capture–emission ratio at a large negative gate bias, $(\tau_c/\tau_c)_{po}$ is the capture–emission ratio at a large positive gate bias, and T is the temperature of carriers in the CNT channels. With $(\tau_c/\tau_c)_{ne} = 15$ and $(\tau_c/\tau_c)_{po} = 12$, the band gap of the CNT is 2 meV. One important issue of the determination of the band gap by using the RTS method is to maintain a small source–drain bias. Because a large electrical field across the CNT may result in carrier heating, the carrier temperature may be higher than the ambient temperature. Figure 2b shows the RTS emission and capture ratio as a function of gate bias for another SWNT-FET¹³ measured at 4.2 K with $V_{ds} = -0.3$ and -0.5 V. The change in the gate-dependence slope at different V_{ds} values shows that carrier heating is indeed a problem in the electrical field range of 5×10^4 V/m. Hence, a small applied electrical field is needed to provide accurate band gap information in the RTS method.

To further confirm the small band gap of the SWNT, differential conductance at zero source–drain bias, shown in Figure 1b, is also used to extract band gap information. The zero-conductance gap gives a gate bias range of about 2.5 V, and from the device structure, a band gap of 6 meV is obtained,¹⁴ which is comparable to that of the previous RTS method. The differential conductance as a function of source–drain bias at different gate biases is shown in Figure 3. The zero-conductance gap at a gate bias of 5 V corresponding to a source–drain bias of 4 meV indicates the small band gap of the SWNT. The temperature-dependent differential conductance with $V_{ds} = 0$ is also obtained as shown in Figure 4. The zero-conductance gap disappears at a temperature of 20 K, which confirms that the band gap of the SWNT is on the order of several millielectronvolts.¹⁵ The zero-bias conductance decreases at 115 K, which shows the metallic characteristics of the SWNT.

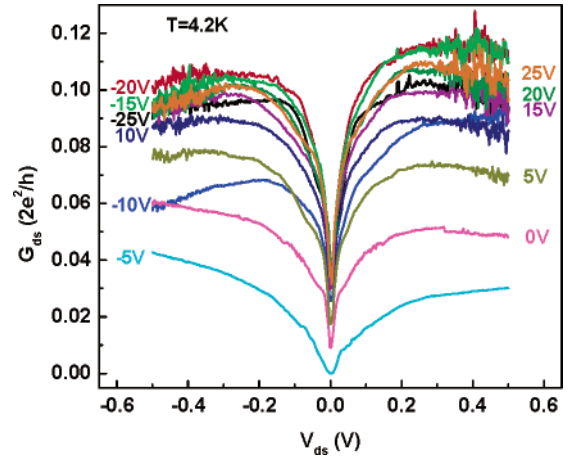


Figure 3. Differential conductance as a function of source–drain bias at different gate biases measured at 4.2 K.

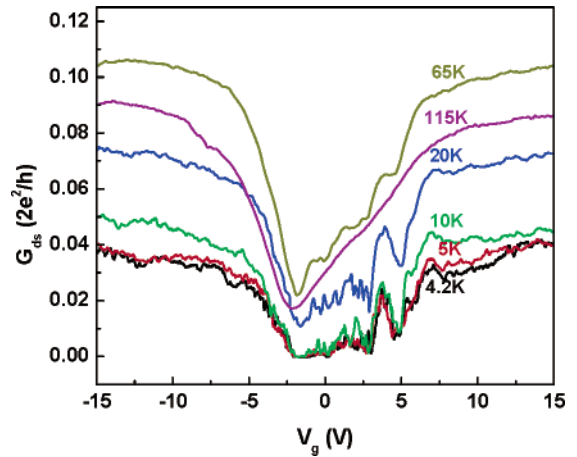


Figure 4. Zero source–drain bias conductances as a function of temperature. The zero-conductance gaps disappear at a temperature of 20 K.

The latter three experimental data support the small band gap of the SWNT obtained from the RTS method. The RTS band gap method is easy to use and accurate because it uses simple $I-V$ measurements instead of a complicated far-infrared optical setup. Compared to the other electrical methods, no detailed device parameters, such as device geometry, CNT band gap, doping, and Schottky barrier heights, are needed for accurate modeling to extract the band gap information. The RTS for band gap extraction has no effect on the contact problem because the band gap is acquired by comparing the defect level to the Fermi level in the SWNT. Furthermore, defects may be intentionally created by hot carrier injection or by creating/localizing defects by other means, such as atomic force microscopy (AFM) and scanning tunneling microscopy (STM). For an emission–capture time constant ratio of 2 orders of magnitude, a maximum band gap of 4 meV can be measured with a carrier temperature of 4.2 K. At higher ambient temperature, a larger band gap range can be extracted using the RTS method.

A hysteresis effect is also observed in the same CNT-FET. These curves were taken from -15 to 15 , -20 to 20 , and -30 to 30 V forward and backward for a V_{ds} of -0.2 V. A substantial shift of the threshold of the CNT-FET is

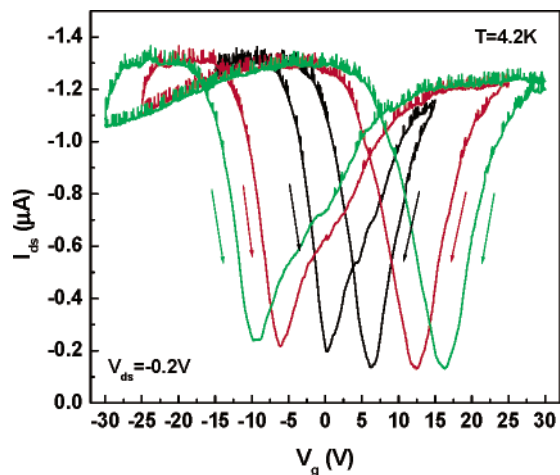


Figure 5. Hysteresis effect of the ambipolar CNT-FET with its RTS. The hysteresis is believed to be due to long-lifetime water molecules and/or mobile charges located in the gate oxide, whereas the RTS is due to the defect with a relatively short lifetime and trapping and detrapping at the interface.

shown in Figure 5. The shift of the threshold is due to the water molecules in the carbon nanotube¹⁶ and/or the charging/discharging of mobile charges in the gate oxide.⁷ Different from the RTS defect state, this kind of trapping event has a much longer lifetime, which results in repeatable hysteresis characteristics. It is interesting that the RTS occurs in each of the I - V curves and it shifts simultaneously with the hysteresis I - V characteristics. In each curve, the up and down probabilities at large positive and negative biases are almost the same, indicating that the RTS signals are quite robust and are not quite affected by other parameters such as mobile charges and water molecules. The water molecules and the mobile charges shift the gate bias dependence of the CNT-FET capacitance without changing the difference between the Fermi energy of CNT and the RTS defect level, thus they do not affect the RTS method of characterization.

In summary, CNT-FETs are extremely sensitive to individual charges, including defect charges with relatively short times (RTSs) and mobile charges/water molecules with long lifetimes (shift of threshold voltage), because of their ultrasmall diameters. The ambipolar random telegraph signal

with both electron and hole conduction was first observed in an ambipolar CNT-FET. Because RTS can acquire CNT Fermi energy information, novel RTS nanometrology was used to extract an ultrasmall CNT band gap with potentially high accuracy. The band gap obtained by the RTS method was consistent with the band gap obtained from the zero-bias differential conductance method and the temperature-dependent conductance method. The work demonstrates the great potential of using RTS phenomena in one-dimensional nanoscale devices as a novel nanometrology technique.

Acknowledgment. This work was supported in part by the MARCO Focus Center on Functional Engineered Nano Architectonics (FENA).

References

- (1) *Carbon Nanotubes: Synthesis, Structure, Properties, and Applications*; Dresselhaus, M. S., Dresselhaus, G., Avouris, P., Eds.; Springer: Berlin, 2001; Vol. 80.
- (2) Kane, C. L.; Mele, E. J. *Phys. Rev. Lett.* **1997**, *78*, 1932.
- (3) Crespi, V. H.; Cohen, M. L.; Rubio, A. *Phys. Rev. Lett.* **1997**, *79*, 2093.
- (4) Ugawa, A.; Rinzler, A. G.; Tanner, D. B. *Phys. Rev. B* **1999**, *60*, R11305.
- (5) Zhou, C.; Kong, J.; Dai, H. *Phys. Rev. Lett.* **2000**, *84*, 5604.
- (6) Cao, J.; Wang, Q.; Rolandi, M.; Dai, H. *Phys. Rev. Lett.* **2004**, *93*, 216803-1.
- (7) Radosavljevic, M.; Freitag, M.; Thadani, K. V.; Johnson, A. T. *Nano Lett.* **2002**, *2*, 761.
- (8) Liu, F.; Bao, M. Q.; Kim, H. J.; Wang, K. L.; Liu, X. L.; Li, C.; Zhou, C. W. *Appl. Phys. Lett.* **2005**, *86*, 163102.
- (9) Kong, J.; Soh, H. T.; Cassell, A. M.; Quate, C. F.; Dai, H. J. *Nature* **1998**, *395*, 878.
- (10) Due to the hysteresis effect shown in Figure 5, the transport characteristics in Figure 2 shift from that of Figure 1.
- (11) Misewich, J. A.; Martel, R.; Avouris, Ph.; Tsang, J. C.; Heinze, S.; Tersoff, J. *Science* **2003**, *300*, 783.
- (12) Taur, Y.; Ning, T. H.; *Fundamentals of Modern VLSI Devices*; Cambridge University Press: Cambridge, U.K., 1998.
- (13) The SWNT-FET is a p-type SWNT-FET with exactly the same device geometry. However, no electron conducting can be observed because of a large band gap.
- (14) Here we used an efficiency factor of 2.5 meV/V obtained from Coulomb blockade data.
- (15) However, it is difficult to extract accurate band gap information from the temperature-dependent conductance method because the band gap is on the order of the thermal excitation energy.
- (16) Kim, W.; Javy, A.; Vermesh, O.; Wang, Q.; Li, Y.; Dai, H. J. *Nano Lett.* **2003**, *3*, 193.

NL050578C